Published online 23 January 2013 *Nucleic Acids Research, 2013, Vol. 41, No. 5* ***3257–3273***
doi:10.1093/nar/gkt007

Development of bis-locked nucleic acid (bisLNA) oligonucleotides for efficient invasion of supercoiled duplex DNA

Pedro M. D. Moreno[1], Sylvain Geny[1], Y. Vladimir Pabon[1], Helen Bergquist[1], Eman M. Zaghloul[1,2], Cristina S. J. Rocha[1], Iulian I. Oprea[1], Burcu Bestas[1], Samir EL Andaloussi[1], Per T. Jørgensen[3], Erik B. Pedersen[3], Karin E. Lundin[1], Rula Zain[1,4], Jesper Wengel[3] and C. I. Edvard Smith[1,*]

[1]Department of Laboratory Medicine, Clinical Research Center, Karolinska Institutet, 141 86 Huddinge, Stockholm, Sweden, [2]Department of Pharmaceutics, Faculty of Pharmacy, Alexandria University, El-Khartoum square, Azareeta, 21 521 Alexandria, Egypt, [3]Department of Physics, Chemistry and Pharmacy, Nucleic Acid Centre, University of Southern Denmark, 5230 Odense, Denmark and [4]Childhood Cancer Research Unit, Department of Women's and Children's Health, Karolinska Institutet, 171 76 Stockholm, Sweden

Received November 26, 2012; Revised December 21, 2012; Accepted December 30, 2012

ABSTRACT

In spite of the many developments in synthetic oligonucleotide (ON) chemistry and design, invasion into double-stranded DNA (DSI) under physiological salt and pH conditions remains a challenge. In this work, we provide a new ON tool based on locked nucleic acids (LNAs), designed for strand invasion into duplex DNA (DSI). We thus report on the development of a clamp type of LNA ON—bisLNA—with capacity to bind and invade into supercoiled double-stranded DNA. The bisLNA links a triplex-forming, Hoogsteen-binding, targeting arm with a strand-invading Watson–Crick binding arm. Optimization was carried out by varying the number and location of LNA nucleotides and the length of the triplex-forming versus strand-invading arms. Single-strand regions in target duplex DNA were mapped using chemical probing. By combining design and increase in LNA content, it was possible to achieve a 100-fold increase in potency with 30% DSI at 450 nM using a bisLNA to plasmid ratio of only 21:1. Although this first conceptual report does not address the utility of bisLNA for the targeting of DNA in a chromosomal context, it shows bisLNA as a promising candidate for interfering also with cellular genes.

INTRODUCTION

The availability of the complete human genome and the ongoing determination of sequence variability, both disease and non-disease causing, provide the appropriate landscape for developments in the gene manipulation field. For this purpose, DNA- and RNA-targeted molecules have been used with several different outcomes. RNA targeting through the use of antisense single-strand (ss) oligonucleotides (ONs) or small interfering RNA (siRNA) has been more generally applied to achieve down-regulation of gene expression (1). DNA targeting, in this respect, could have a wider applicability functioning not only in gene down-regulation but also for up-regulation and even for permanent gene correction. Sequence-specific double-strand (ds) DNA-binding ONs and polyamides have been developed for these purposes. ssONs have, in this respect, been found to possess the capacity to bind to polypurine–polypyrimidine regions of dsDNA in a sequence-specific manner by targeting the dsDNA major groove and forming Hoogsteen or reverse Hoogsteen hydrogen bonds between bases (2,3). This mode of binding creates

*To whom correspondence should be addressed. Tel: +46 8 585 838 00; Fax: +46 8 585 836 50; Email: edvard.smith@ki.se
Present address:
Pedro M. D. Moreno, INEB-Instituto de Engenharia Biomédica, Universidade do Porto, Rua do Campo Alegre, 823, 4150-180 Porto, Portugal.

The authors wish to be known that, in their opinion, the first two authors should be regarded as joint First Authors.

© The Author(s) 2013. Published by Oxford University Press.
This is an Open Access article distributed under the terms of the Creative Commons Attribution Non-Commercial License (http://creativecommons.org/licenses/by-nc/3.0/), which permits unrestricted non-commercial use, distribution, and reproduction in any medium, provided the original work is properly cited.

a triple-helix structure, and the ONs with this capacity are referred to as triplex-forming ONs (TFOs). TFOs have been used in different gene-targeting approaches such as gene down-regulation by interfering with transcription initiation (4–6) or transcription elongation (7,8), gene activation (9,10) and site-directed mutagenesis and recombination (11,12). In the field of nucleic acid-based dsDNA-binding compounds, numerous chemistries have been used, achieving different modes of binding. Some examples are TFOs based on 2′-*O*-methyl and 2′-*O*-aminoethyl chemistry (13,14), PNA (peptide nucleic acid)-based ONs targeting dsDNA through triplex formation or strand displacement (15) and LNA (locked nucleic acid)-based ONs also used as TFOs (16–18) and as tools for strand displacement (19,20).

Despite these efforts, targeting of a specific position on an endogenous gene by the use of nucleic acids/ONs remains a challenge. The limitations for nucleic acid-based anti-gene molecules have been related to binding affinity, specificity, accessibility and cellular uptake and ON stability *in vitro* and *in vivo*. Exclusive for the TFO approach is the need for polypurine–polypyrimidine target stretches. However, such sequences are frequently found in eukaryotic genomes mainly in promoter regions but also available in intronic regions (21–23). Interestingly, polypurine–polypyrimidine chromosomal DNA sequences that possess mirror symmetry can also form a triple-helix structure in an intramolecular manner where part of the polypurine or polypyrimidine strand acts as the triplex-forming third strand (24,25). Binding to dsDNA through Watson–Crick base pairing by a strategy of dsDNA invasion is not hampered by sequence restrictions. It does suffer, however, from a much more complex and slower mode of action where the anti-gene ON needs to access its corresponding chromatin region and subsequently displace one of the DNA strands to form Watson–Crick base pairing with its cognate sequence. This mode of targeting, while promising, has not yet been developed into a widely used tool (15,19,26–29).

As mentioned above, LNA ONs have been used in anti-gene strategies based on both TFO and dsDNA invasion mechanisms. An LNA nucleotide contains a methylene bridge connecting the 2′ to 4′ positions of the ribose, which leads to a conformational restriction of the ribose sugar. This in turn results in increased hybridization affinity towards DNA and RNA (30). These properties seem to be useful also in a TFO context. LNA-substituted TFOs show an increased triplex thermostability, although a fully LNA-substituted TFO hampers triplex stability (31,32). Moreover, and likely owing to the fact that a methylated cytosine is the standard building block in LNA synthesis, increased affinities are also seen at neutral pH, which is of importance for the TFO parallel motif (homopyrimidine-type TFOs) and for the efficient binding under intracellular conditions (16,33).

To further develop the ON-based anti-gene approach, we sought to harness the positive contributions of LNA modifications, both for TFO- and duplex-invasion modes, and incorporate them in a clamp type of construct, thereby creating a bisLNA molecule. The concept of clamp constructs was proposed before and its efficacy shown for the binding to single-stranded DNA or RNA (34–36). This concept was further explored in the development of bisPNAs, demonstrating that ONs with this design have enhanced hybridization properties to dsDNA (37,38). In a series of elegant publications, it was demonstrated that the likely mechanism was an initial TFO binding, followed by duplex-strand invasion (39,40), that the substitution of cytosines for pseudo-deoxycytosines significantly improved hybridization at physiological pH (37) and that an extension resulting in a tail-clamp construct further improved hybridization properties (41). It was also reported that increasing the ionic strength strongly favours triplex formation over invasion, as the latter is severely inhibited by cations, and that isolated triplex complexes can be converted to specific invasion complexes without dissociation of the Hoogsteen bonds in the PNA triplex (15,42). This design has, to the best of our knowledge, so far not been sufficiently explored for LNA. Thus, while Hertoghs *et al*. (43) already in 2003 reported on a 9-mer bisLNA, this ON was less efficient than the corresponding LNAs lacking a TFO region in binding to plasmids. We now demonstrate that optimizing design and composition of bisLNA molecules is crucial for obtaining ONs with advantageous properties as compared with LNA oligomers devoid of a TFO portion. Importantly, we for the first time conclusively demonstrate the capacity of LNA molecules to achieve duplex invasion of supercoiled DNA under ion concentration and pH similar to the intracellular nuclear environment. Thus, bisLNA constitutes a highly promising tool for achieving chromosomal target recognition, enabling the development of efficient anti-gene strategies.

MATERIALS AND METHODS

Oligonucleotides

Mixmer LNA/DNA ON strands were synthesized by solid phase phosphoramidite chemistry on an automated DNA synthesizer in 1.0 mmol synthesis scale. Purification to at least 80% purity of all modified ONs was performed by RP-HPLC or IE-HPLC, and the composition of all synthesized ONs was verified by MALDI-MS analysis recorded using 3-hydroxypicolinic acid as a matrix. The ONs used in this work are presented in Table 1.

Plasmids

The pEGFPLuc/G6 is based on previously reported G site-containing plasmids (44). The G6 version contains six G sites with two bases in between. The pDel-1 plasmid containing the full human *MYC* promoter (45) was obtained from Addgene (Cambridge, USA). To study the influence of the flanking region surrounding the bisLNA-binding site, we also created plasmids pEGFPLuc-bisBSf and pEGFPLucbisBSr. To do this, we inserted 35 bases including the bisLNA target site from pDel-1, between the NheI and AgeI restriction sites in the 5′ untranslated region of the reporter construct in the pEGFPLuc plasmid (Clontech). Table 2 presents a list of the used plasmids together with their corresponding target sites.

Table 1. LNAs and the corresponding sequences used in this work

Group 1 ONs	Target sequence: 5′-AAGAAGAAAA-3′
bisLNA-20	Cy3-tTcTtCtTtT-ctctc-tTtTcTtCtT
bisLNA-20a	Cy3-tTcTtCtTtT-ctctc-ttttcttctt
bisLNA-20b	Cy3-ttcttctttt-ctctc-tTtTcTtCtT
bisLNA-20c	Cy3-tTcTtCtTtT-s18-tTtTcTtCtT
bisLNA-20d	Cy3-tTcTtCtTtT-s18-tTtTcTtCtT (fully phosphorothioated)
bisLNA-20e	Cy3-tTcTtCtTtT-s18 ± s9-tTtTcTtCtT
TFO-LNA-20	Cy3-tTcTtCtTtT
WC-LNA-20	Cy5-tTtTcTtCtT
Group 2 ONs	Target sequence: 5′-*GCAGAGGGCGTGGG*GGAAAAGAAAAAAGA-3′
bisLNA-m30	Cy3-cCtTtTcTtTtTtCt-tctct-TcTtTtTtCtTtTcC
bisLNA-m44	Cy3-CcTtTtCtTtTtTcT-tctct-tCtTtTtTcTtTtCcCccAcgCccTctGc
bisLNA-m44a	Cy3-CcTtTtCtTtTtTcT-tctct-TcTtTtTtCtTtTcCCccAcgCccTctGc
bisLNA-m44b	Cy3-cCtTtTcTtTtTtCt-tctct-TcTtTtTtCtTtTcCCccAcgCccTctGc
bisLNA-m44c	Cy3-CcTtTtCtTtTtTcT-tctct-TcTtTtTtCtTtTccCccAcgCccTctGc
bisLNA-m44d	Cy3-cCtTtTcTtTtTtCt-tctct-tCtTtTtTcTtTtCcCccAcgCccTctGc
bisLNA-m44e	Cy3-CcTtTtCtTtTtTcT-tctct-tCtTtTtTcTtTtCcCccACgCCcTCtGC
bisLNA-m44-3t	Cy3-tTtCtTtTtTcT-tctct-tCtTtTtTcTtTtCcCccAcgCccTctGc
bisLNA-m44-7w	Cy3-CcTtTtCtTtTtTcT-tctct-tCtTtTtTcTtTtCcCccAcgC
WC-LNA-m30	Cy5-TcTtTtTtCtTtTcC
WC-LNA-m44	Cy5-tCtTtTtTcTtTtCcCccAcgCccTctGc
TFO-LNA-m30/44	Cy3-cCtTtTcTtTtTtCt
Group 3 ONs	Target sequence: 5′-*GGGAAAAAGAAC*GGAGGGAGGGA-3′
bisLNA-m(P2)37	Cy3-CcTcCcTcCcT-tctctc-TcCcTcCcTcCgTtCtTtTtCcCgCc

LNA bases are in capital letters; DNA bases in small letters; linker sequence/region is underlined; s18 = hexaethylene glycyl linker; s18 + s9 = hexaethylene glycyl extended with a triethylene glycyl linker; target sequence of group 2 and 3 LNAs shown in italic corresponds to the complementary region of the extended Watson–Crick arm of bisLNA-m44. Rational behind designations: m indicates a bisLNA targeting a *MYC* sequence, numbers correspond to number of nucleotides without those in the linker, t and w indicate the nature of the altered arm (TFO or WC, respectively) followed by the reduced number of nucleotides in the arm.

Table 2. Plasmids used in this study and respective target sequences

Plasmid	Binding site sequence present
G6	5′-AAGAAGAAAA-3′
pDel-1	5′-*GCAGAGGGCGTGGG*GGAAAAGAAAAAAGA-3′
pDel-1/P2	5′-*GGGAAAAAGAAC*GGAGGGAGGGA-3′
pDel-1 mut 1G	5′-*GCAGAGGGCGTGGG*GGAAAAGGAAAAAGA-3′
pDel-1 mut 1C	5′-*GCAGAGGGCGTGGG*GGAAAAGCAAAAAGA-3′
pDel-1 mut 2G	5′-*GCAGAGGGCGTGGG*GGAAAAGGAAAAGGA-3′
pDel-1 mut 2C	5′-*GCAGAGGGCGTGGG*GGAAAAGCAAAACGA-3′
pEGFPLu-c-bisBSf	5′-*GCAGAGGGCGTGGG*GGAAAAGAAAAAAGA-3′
pEGFPLu-c-bisBSr	5′-*GCAGAGGGCGTGGG*GGAAAAGAAAAAAGA-3′

In the case of multiple binding sites, only the single unit sequence is presented, as the target sequence is always the same.
Italic letters represent the specific binding segment for the extended Watson–Crick arm of bisLNAs, the remaining sequence being the one targeted by the TFO arm.
Underlined bases correspond to mutated bases in relation to the original plasmid used.

Plasmid hybridizations

The G6 plasmid at final concentration of 100 ng/μl was hybridized with different ON constructs, at different final ON concentrations (namely 0.05, 0.15, 0.45, 1.35, 4.05 and 12 μM, corresponding to a bisLNA:plasmid ratio of, respectively, 2.5, 7.6, 22.7, 68.2, 204.6 and 613.6) in low salt phosphate buffer at pH 5.8 (final buffer composition: 20 mM $NaPO_4$, 20 mM NaCl, pH 5.8) in a final volume of 10 μl. Hybridizations were carried out at 37°C in an oven incubator for 16–20 h.

pDel-1 plasmids and pEGFP-based plasmids containing a binding site from the human genomic *MYC* region were incubated under the same conditions as above (same bisLNA concentrations used) except for that an intranuclear buffer was used (final buffer composition: Tris-acetate 50 mM, (pH 7.3–7.4), 120 mM KCl, 5 mM NaCl, 0.5 mM Mg-acetate). Hybridizations were carried out at 37°C for 16 or 72 h. For pDel-1, the bisLNA:plasmid ratios, according to the concentration of bisLNA, were, respectively, 2.4, 7.1, 21.4, 64.2, 192.9 and 578.6.

Agarose Gel Electrophoresis Fluorescent Binding Assay (GEFA)

A standard curve for quantitatively analysing the binding was prepared previous to the gel run by incubating the appropriate Cy3/Cy5-ON with a complementary ON (cON) containing a single target site. The ONs were hybridized at room temperature for ≥16 h.

An amount of 500 ng of plasmid was loaded in the lower row of wells of an 0.8% agarose gel (0.5× TBE) and ran for 45 min at 80 V in a Horizon 58 gel system (Biometra). Known amounts of labelled ON hybridized to cON were subsequently loaded in an upper row of wells of

the same gel for the generation of standard curves. The gel was further run for an additional 15 min. Plasmid-bound ON and the standard curve ON were detected by the emitted fluorescence in a VersaDoc system (BioRad) and analysis and quantifications done using the QuantityOne software (BioRad). To verify equal loading of plasmid DNA in each well, the gel was stained *a posteriori* with EtBr and the signal used for normalization.

S1 nuclease assay

An amount of 250 ng of hybridized plasmid was incubated with 24 units of S1 enzyme (Promega) in a total volume of 11 µl at 4°C for 6 min. The reaction was stopped by the addition of 3 µl 500 mM EDTA. A volume of 1.5 µl of the final solution was loaded and ran in a 0.9% agarose gel (1× TAE or 0.5× TBE) containing SybrGold (Molecular Probes, Invitrogen). The same detection system and analysis software as described above were used to calculate the fractions of linear/nicked (n) and supercoiled (sc) plasmid present in each sample.

Restriction digestions and PAGE Electrophoretic Mobility Shift Assay (P-EMSA)

An amount of 250 ng of hybridized G6 plasmids was digested with HpaI and SspI (FastDigest, Fermentas). The digested plasmid was then loaded in a Novex 4–20% TBE polyacrylamide gel (Invitrogen) and stained after the gel run with SybrGold (Molecular Probes, Invitrogen). Detection and analysis was done as described above.

Restriction digestions and Agarose Electrophoretic Mobility Shift Assay (A-EMSA)

An amount of 500 ng of hybridized plasmid pDel-1 (16 h hybridizations with 12 µM LNA) was digested with XhoI and SmaI (FastDigest, Fermentas). The digested plasmid was then loaded in a freshly made 2% agarose TBE gel containing 2 mM $MgCl_2$. The gel electrophoresis was performed at 4°C (120 V, 1 h 45 min) and stained after the gel run with SybrGold (Molecular Probes, Invitrogen).

Chemical probing

Plasmid pEGFPLuc-bisBSf (4 µg) was first incubated in intranuclear buffer (Tris acetate 50 mM, pH 7.3–7.4, 120 mM KCl, 5 mM NaCl, 0.5 mM magnesium acetate) at 37°C for 72 h in the absence or presence of either bisLNA-m44 or bisLNA-m30 (4–12 µM, final volume 40 µl).

DNA chemical modification of supercoiled plasmids was then performed by adding 2% chloroacetaldehyde (CAA) to the plasmid solution (containing 1 µg of plasmid, final volume 20 µl), and the reaction was allowed to proceed for 30 min at 37°C, followed by isolation of the DNA using miniprep columns (Qiagen). The isolated DNA was then linearized using SacI FastDigest (Fermentas) for 1 h at 37°C and subjected to alkaline treatment (1 mM NaOH, 30 min, 90°C) followed by neutralization using Tris-HCl (4 µl, 100 mM, final volume 30 µl).

DNA chemical modification of linear plasmids was performed after linearization of the LNA hybridized (or control) plasmid (1 µg) using SacI FastDigest (Fermentas) for 1 h at 37°C (final volume 15 µl). The linearized plasmid was then modified by adding 2% CAA (final volume 20 µl), and the reaction was allowed to proceed for 30 min at 37°C. The DNA was isolated using miniprep columns (Qiagen), followed by alkaline treatment as described above.

The CAA-modified plasmids were used as templates for the primer extension reactions using [γ-^{32}P]ATP 5′-labelled forward 5′-AAA TGG GCG GTA GGC GT-3′ or reverse 5′-AAC TTG TGG CCG TTT ACG TC-3′ primers. Labelling of primers was performed using T4 polynucleotide kinase (Fermentas) according to the manufacturer's protocol and then purified using QIAquick Nucleotide Removal Kit (QIAGEN). A primer extension mix [2 mM $MgCl_2$, 3 U Taq polymerase (Fermentas), 2.5 nM primer, 2 mM of each dNTP] was added to ~100 ng template, and the reaction was carried out according to the following conditions: 10 min at 94°C, 29 cycles of 1 min at 94°C, 2 min at 45°C, 3 min at 72°C and finally 10 min at 72°C. Plasmids incubated under similar conditions, but not treated with CAA, were used as controls. Sequencing ladders were prepared by using plasmids (100 ng) cleaved by SacI and NdeI Fast Digest enzymes (Fermentas) as templates for the primer extension reaction in the presence of dideoxynucleotides (4.5 mM ddATP, 2.5 mM ddCTP, 1.0 mM ddGTP and 2.4 mM ddTTP). All samples were analysed using denaturing polyacrylamide gel electrophoresis (6%, 7 M urea, 0.5 mm) in buffer (1× TBE) at room temperature and 1200 V, 32 mA, 4 h. A Molecular Imager FX and the Quantity One software (BioRad) were used for scanning and analysis of the gel.

Thermal melting analysis

Absorbance versus temperature profile measurements were carried out with a Varian Cary 300 Bio spectrophotometer, in quartz cells of 1 cm path length. The variation of UV absorbance with temperature was monitored at 260 nm. Preparation of samples was carried out as follows. The LNA and the target ONs (G site target ON: 5′-TCG ATA CGC GAA GAA GAA AAC TGC GTA CGA; *MYC* site target ON: 5′-CAA AGC AGA GGG CGT GGG GGA AAA GAA AAA AGA TCC TCT CTC GCT AAT C; binding sites are underlined) were mixed from stock solutions to make up a final concentration of the triplex of 3 µM in a solution of sodium phosphate (20 mM) at pH 5.8 for the 10-mer bisLNAs, and sodium phosphate (20 mM) at pH 7.3 for the 15-mer bisLNAs. The samples were hybridized at room temperature for 2 h. The dissociation was recorded by heating to 90°C at the rate of 0.2°C min^{-1}, and the association was recorded by cooling down to 20°C at 0.2°C min^{-1}. The datapoints were collected every 0.1°C. Varian Cary WinUV software version 3 was used to determine the melting temperatures (T_m). T_m values were determined from the first derivatives of the observed thermal transitions after smoothing of the curves. Reported values are the average of at least two experiments.

RESULTS

Binding of bisLNAs to supercoiled DNA

We set out to investigate the binding efficiencies of LNA ONs to supercoiled plasmid DNA. Initially, we evaluated the binding of 10-mer ONs (Table 1) to a plasmid containing six binding sites (BSs) (G6 plasmid) composed of an uninterrupted 10 nt purine stretch with a 2 nt interval between each site (44). The binding was evaluated at non-physiological binding conditions, using low salt and low pH. A 40 mM salt concentration was used, as it gave higher binding of bisLNA (data not shown) and the pH was below 7 (pH 5.8) to allow for cytosine protonation and thus improved pyrimidine-based TFO binding.

We compared the binding efficiencies between an LNA ON binding only in Watson–Crick fashion (WC-LNA-20), an LNA ON capable of binding in parallel Hoogsteen mode (TFO-LNA-20) and an LNA ON composed of the above mentioned WC- and TFO-LNAs joined by five DNA bases (bisLNA-20). These five DNA extra bases are non-complementary to the BSs and act as a linker sequence, creating a clamp-type LNA ON as presented in Figure 1a. Moreover, we co-incubated TFO-LNA-20 and WC-LNA-20 with the plasmid to test the contribution of the linker.

After incubation with plasmid G6 (6 BSs) at 37°C for ~16 h, binding was verified by running the plasmid in an agarose gel and compared with a standard curve. Because all ONs were Cy3- or Cy5-labelled, the signal from the hybridized plasmid could be compared with the signal from known amounts of LNA ONs in order to quantitatively determine the amount of LNA still bound after the gel electrophoresis (Supplementary Figure S1 shows examples of GEFA results).

Under standard agarose gel electrophoresis conditions, we could not detect any binding of TFO-LNA-20 or WC-LNA-20 when used separately (data not shown), but binding was observed when co-incubating both arms together with the plasmid. Around 10% of saturated binding for TFO-LNA-20 (Cy3 signal) and ~28% for WC-LNA-20 (Cy5 signal) were reached at the highest concentration used (12 μM). This suggested increased stabilization when adding the unlinked TFO- and the WC-arms at the same time. However, the strongest effect was, as expected, seen when we used the two arms joined by a linker-DNA sequence, creating the bisLNA-20. In this case, 50% binding was achieved already at 0.45 μM, although the detected maximum binding did not increase beyond 65% [Figure 1b-(i) and Supplementary Figure S1].

We also used a fine-tuned S1 nuclease assay (20) to quantify the amount of double-strand invasion (DSI) achieved, which should also reflect the binding efficiencies of the constructs. This assay is based on the properties

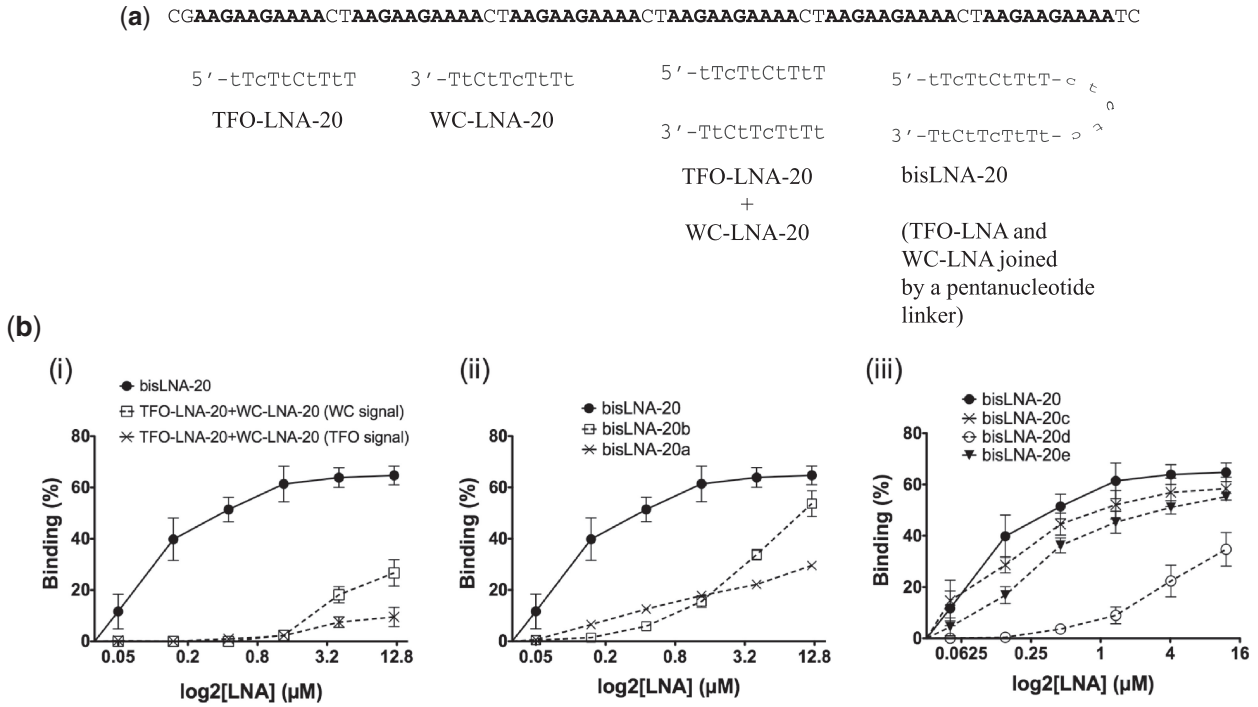

Figure 1. LNA-targeting plasmids with six consecutive binding sites. (**a**) Target sequence in the plasmid with six binding sites (BS in bold) (separated by two bases in between), and schematic representation of the bisLNA-20 construct and its TFO- and Watson–Crick (WC) arm components. (**b**) Quantification of different bisLNA constructs using the GEFA assay. Concentrations used ranged from 0.05 to 12 μM and hybridizations were done in low salt phosphate buffer (pH 5.8) at 37°C for 16—20 h. (**i**) Comparison between constructs bisLNA-20 and TFO-LNA-20 co-incubated with WC-LNA-20. The two curves obtained correspond to the independent fluorescent signals coming from either TFO-LNA-20 (Cy3 signal detected) or WC-LNA-20 (Cy5 signal detected). The two different signals allow to quantify how much of each construct is bound to the plasmid independently of each other, despite of being co-incubated. (**ii**) Comparison between constructs with different LNA/DNA composition in the TFO- or WC arm. (**iii**) Comparison between bisLNA constructs having different linker compositions.

of the S1 nuclease enzyme, which specifically cuts ss regions of DNA. When DSI occurs through Watson–Crick binding of the complementary DNA strand, a region of ssDNA is produced. The extent of single-strand cleavage using S1 nuclease can then be correlated with the ability of an LNA ON construct to invade dsDNA (Supplementary Figure S2). Cleavage of the ssDNA region was evaluated by the amount of super-coiled (sc) plasmid lost owing to conversion to a nicked (n) or linear (l) form.

In this assay, as expected, we did not obtain any DSI by using the TFO-LNA-20, but with the WC-LNA-20 it was possible to reach a maximum of 47% at the highest concentration. When co-incubating unlinked TFO-LNA-20 and WC-LNA-20, we obtained a higher DSI reaching ~68% (Supplementary Figure S3). The use of a clamp type of LNA, the bisLNA-20, is, however, clearly superior as compared with the non-linked LNA constructs, with major differences seen at lower concentrations, where 50% DSI was reached already at 0.15 μM and a maximum of 87% at the highest concentration used. This demonstrates the improved efficiency of such constructs in binding to supercoiled plasmid DNA.

Effect of LNA / DNA composition on each arm of the bisLNA construct

We next wanted to test the influence of each arm in the bisLNA construct in terms of their LNA / DNA composition. With this in mind, we tested two additional constructs, bisLNA-20a and bisLNA-20b, where all the LNA bases were substituted with DNA bases in either the Watson–Crick arm or in the TFO arm, respectively, while keeping 50% LNA content in the opposite arm (Table 1).

As seen in Figure 1b-(ii), bisLNA-20b having a 'full DNA' TFO arm had severely reduced binding to plasmid DNA as measured by the GEFA. At 0.45 μM concentration, where there is ~50% binding of the full bisLNA construct (bisLNA-20), we only achieved ~6% binding of bisLNA-20b. Maximum binding at 12 μM was, however, 54%. In the case where we used a construct with a 'full DNA' Watson–Crick arm, (bisLNA-20a), a marked reduction in the binding was seen. At 0.45 μM, 13% binding was achieved, i.e. higher than bisLNA-20b, while maximum binding was lower than that obtained with bisLNA-20b. In conclusion, having a 50% LNA-substituted bisLNA, with LNA both in the TFO- and Watson–Crick arm, is crucial for efficient DSI.

Effect of the linker region connecting the arms of the bisLNA construct

We further tested the effect of non-nucleotide-based linkers on the efficiency of the bisLNA-20 binding to plasmid DNA. The pentanucleotide linker was chosen initially on the basis of earlier experiments done by Prakash and Kool (46). We thus substituted the pentanucleotide linker found in construct bisLNA-20 with a 1× HEG (bisLNA-20c) of 20 atoms in length or a 1× HEG–TEG (bisLNA-20e) of 31 atoms in length. The pentanucleotide linker, on the sole basis of atom count, would correspond to 31 atoms (six atoms per nucleotide). However, while the HEG/TEG linkers are considered to be flexible, the nucleotide-based linker should have a more constraint structure.

As seen in Figure 1b-(iii), the GEFA showed that bisLNA-20 was still the best construct despite only a marginal advantage over bisLNA-20c. The bisLNA-20e construct, with the longer flexible linker region, was, however, significantly less efficient. This result seems to indicate that having a flexible linker even with roughly the same atom length as the pentanucleotide linker is not optimal. The shorter linker may correspond to the optimal length provided by the pentanucleotide linker, which *per se* is more structurally rigid than an ethylene glycol-based chain (47).

We also included in this assay a bisLNA-20 version with a fully modified phosphorothioate (PS) backbone (construct bisLNA-20d). Binding was severely reduced by the presence of the PS linkages, which goes in line with earlier reports (48,49).

bisLNA binding withstands linearization of sc plasmid DNA by enzyme digestion

It has been reported earlier that linear LNAs can only bind to supercoiled DNA, whereby linearization of the supercoiled DNA will provoke dissociation of the previously bound linear LNA (50). To test whether a bisLNA would resist such a 'kick-out' effect, we hybridized the LNA to plasmid DNA followed by digestion with restriction enzymes (REs). The REs were selected to cut in regions flanking the LNA BSs, which allowed us to run a PAGE assay and look for shifts of the BS-containing fragment. As seen in Figure 2, all the bisLNA constructs withstood the plasmid digestion treatment, albeit with variable efficiency, likely correlated to their binding strength. Interestingly, we were also able to distinguish the shifts of the BS-containing fragment depending on the number of bisLNAs or linear LNAs bound (1–6 shifts that are represented by the asterisks in the picture). As expected, bisLNA-20 had the stronger binding judged by the more prominent shift of the BS-containing fragment to the positions corresponding to 5–6 LNAs bound in comparison for example to bisLNA-20b, which at the highest concentration had more prominent shifts of the fragment to positions corresponding to only 4–5 LNAs bound. Neither of the unlinked TFO-LNA-20 nor WC-LNA-20 remained bound, but again, when co-incubating both, we observed weak, but detectable, shifted BS fragments. Nonetheless unlinked TFO-LNA and WC-LNA bound to the same site show a cooperative effect. This could result from local structural effects on the DNA imparted by the joint TFO-LNA and WC-LNA binding, likely related to the C3′-endo configuration usually adopted by ONs containing LNA bases (30).

Unexpectedly, bisLNA-20d (full PS linkages) seemed to have unpredictable effects on the action of the enzymes, as BS fragments were lost with increasing amounts of LNA, while no shifts could be observed.

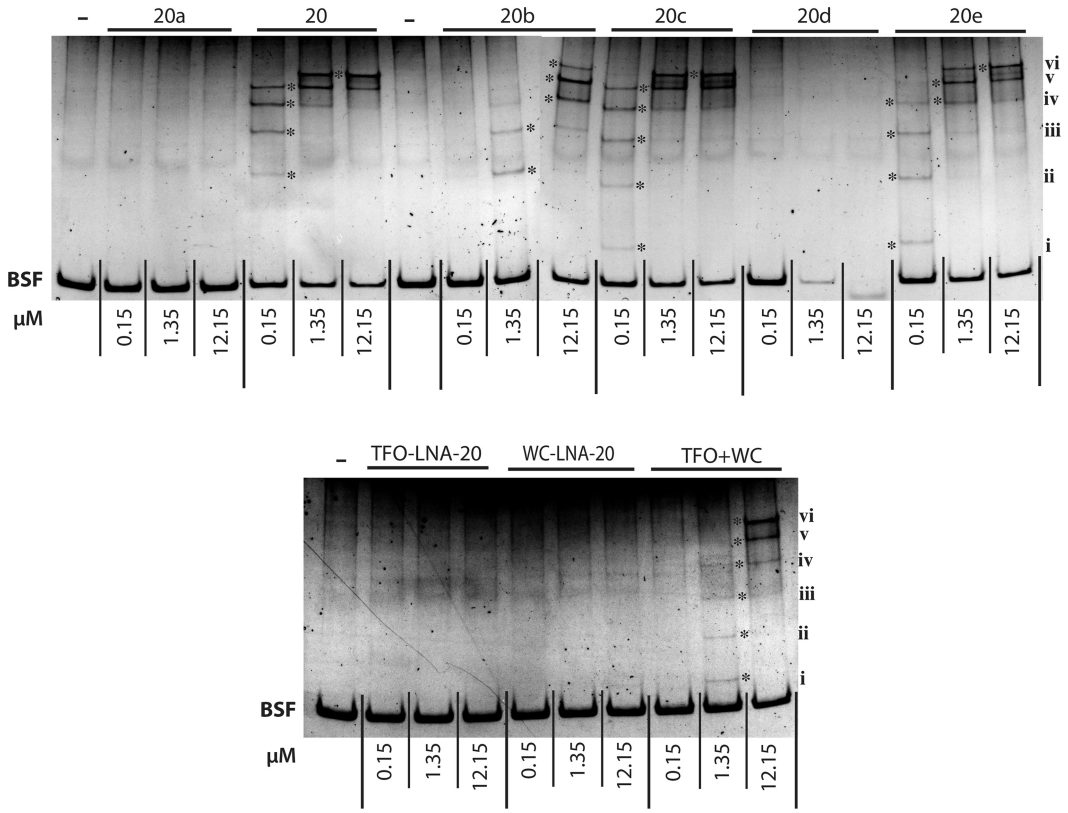

Figure 2. Representative gels showing the PAGE-shift assay after RE digestions of LNA-hybridized plasmid pEGFPLuc/G6. Asterisks indicate the positions of the shifted DNA fragments. The highest shift occurs when the fragment's target sites are saturated and the lowest shift occurs with the occupancy of only a single target site of the fragment. The letters 'i–vi' on the side of the gels represent the number of target sites occupied in each position (ranging from i = 1 to vi = 6). Below position 'i' and indicated by BSF (Binding Site containing Fragment) remains the unbound fraction of the DNA fragment.

A bisLNA targeting a single site

The 10-mer bisLNAs were not effective at targeting a single BS plasmid (data not shown), which was not unexpected owing to the low T_m values calculated for the Watson–Crick arm of the bisLNA (~30°C according to calculations done using LNA Oligo Prediction Tools at http://www.exiqon.com/oligo-tools). Plasmid G6 with six BSs can provide binding facilitation owing to a cooperative effect on bisLNA hybridization. Strand invasion of a first bisLNA provides an adjacent opening of the DNA double helix, allowing facilitated binding of consecutive bisLNAs. In the case of the G1 plasmid, with a single binding site, this does not happen (44).

For the single BS sequence, we therefore increased the length of the bisLNA to 15 nt in each arm, again with ~50% LNA composition (Table 1). A targeting sequence originating from the human *MYC* promoter region was used to test the binding of our new 15-mer bisLNA construct, designated bisLNA-m30. The pDel-1 plasmid contains the full *MYC* promoter with a single complementary sequence to this bisLNA, located at the designated P1 promoter region (Figure 3a).

We again used the quantitative GEFA; however, the incubations were now performed in a physiologically relevant intranuclear buffer in terms of salt concentrations and pH. As seen in Figure 3b(i) and Supplementary Figure S4, we managed to obtain a weak, but still visible, binding of the 15-mer bisLNA-m30 to a single site under physiological salt and pH conditions, observing at the highest concentration tested ~5% LNA bound. This result prompted us to improve on the bisLNA design, which resulted in bisLNA-m44, having an extended Watson–Crick arm with in total 29 bases. The 15-bases-long TFO arm remained unaltered, containing a stretch of 15 uninterrupted pyrimidines. The binding depicted in Figure 3b(i) clearly shows the marked improvement observed in binding efficiency, reaching at the highest value ~35%. We also tested the DSI capacity of both bisLNAs by using the S1 nuclease assay and, as seen in Figure 3b(ii) and Supplementary Figure S4, bisLNA-m44 achieved ~54% DSI, while bisLNA-m30 never reached >5% at the highest concentration tested.

LNA-modified ONs are recognized to have quite long half-lives and their effects, such as in antisense approaches, are observable for periods of >3–5 days and even weeks (51–55). With this in mind, we also tested the effect of prolonged (72 h) incubation on the binding and DSI. We observed [Figure 3b(iii) and Supplementary Figure S4] a dramatic increase of duplex invasion for bisLNA-m44, which reached close to 80% at the highest concentration. The bisLNA-m30 ON, however, did not experience any major changes with the increased incubation time,

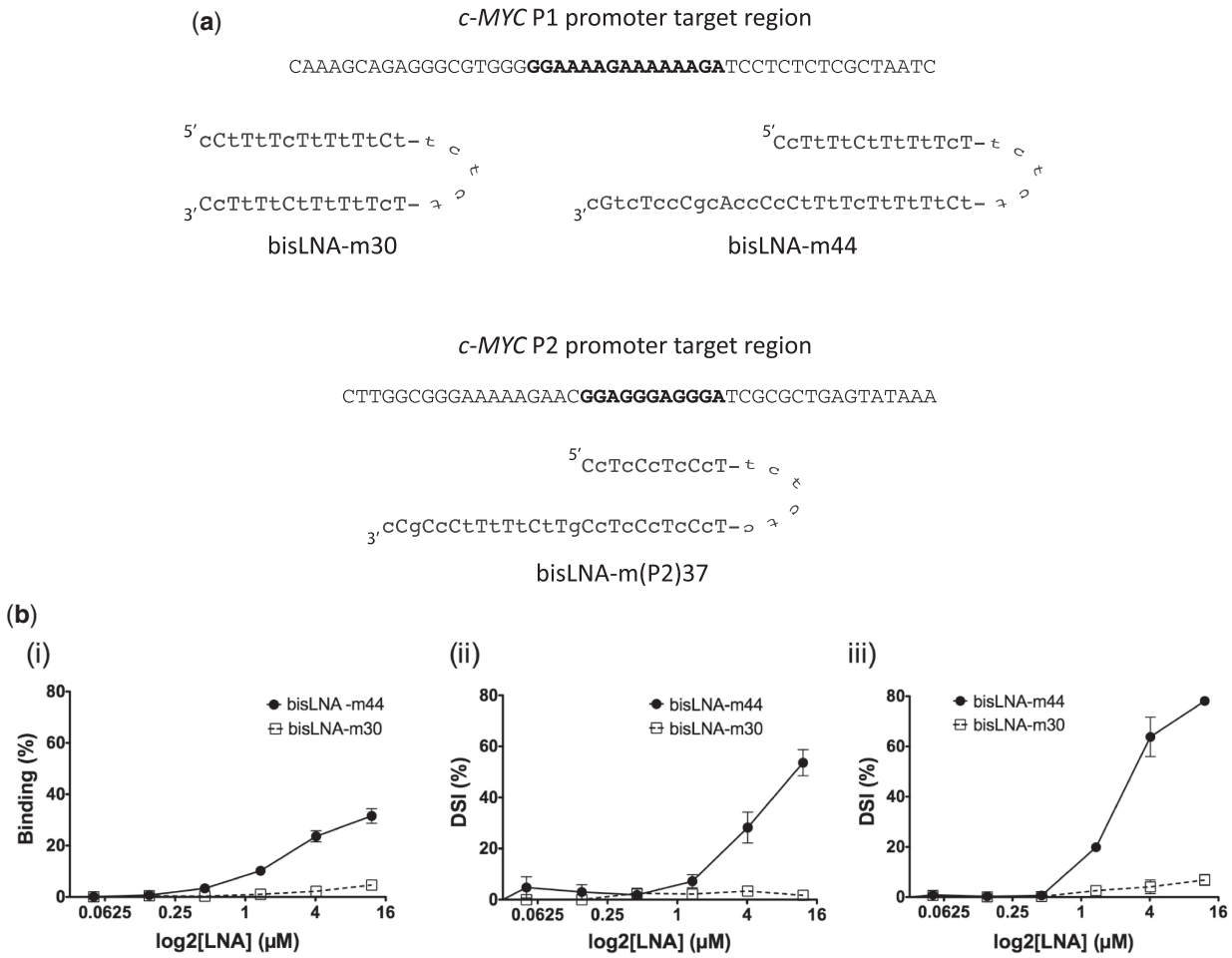

Figure 3. Binding and DSI of bisLNA-m30 and bisLNA-m44 to plasmid pDel-1. (**a**) Sequence of the binding site in the human *MYC* promoter region. In bold is highlighted the original 15-mer target-site sequence. Also represented are the schematic pictures of bisLNA-m30 and the WC-arm-extended bisLNA-m44. (**b**) Quantification of binding by GEFA (**i**), and the DSI determined by the S1 nuclease assay, after overnight hybridizations at 37°C (**ii**), and DSI after hybridizations for 72 h at 37°C (**iii**).

suggesting intrinsic unfavourable properties of this construct for binding to a single site.

The influence of the length of each arm on bisLNA binding to a single site

In an attempt to reduce the length of the bisLNA, we designed two bisLNAs having either a shorter tail or a shorter TFO arm, respectively. Although the 10-mer bisLNAs were too short to be efficient at a single binding site, we thought it was possible to have a tail-clamp bisLNA, shorter than the bisLNA-m44, which could still be more efficient than the 10-mer bisLNAs. As seen in Figure 4a and Supplementary Figure S5a, a construct with a seven bases shorter tail (bisLNA-m44-7w) had a poor DSI capacity (only 15% at 12 μM) as compared with bisLNA-m44 when incubated for 16 h with plasmid pDel-1. In contrast, bisLNA-m44-3t, a construct with three bases shorter TFO, was as efficient as bisLNA-m44 at low bisLNA concentration (16% at 1.35 μM) and slightly more efficient at high concentration (49% at 12 μM). The WC-LNA-m44 lacking the TFO arm was able to perform DSI at high concentration (35% at 12 μM) but is significantly less efficient (6% at 1.35 μM) than bisLNA-m44 (14% at 1.35 μM) and other constructs containing a TFO arm, at low concentration.

The influence of LNA content and position for bisLNA binding and duplex invasion

After strand invasion, both arms of the bisLNA are anticipated to be involved in the triple helix formation. As a result of the triplex formation, the LNA bases of both arms in the bisLNA can either be opposite each other or alternating. So far, no studies have been published on the stability of these different types of triplexes, and we assumed that these structures might influence the DSI rate. To study any difference in terms of the DSI, several versions of bisLNA-tail clamps were synthesized, and the characteristics of these constructs are summarized in Table 3.

Based on the results of the S1 nuclease digestion (Figure 4b and Supplementary Figure S5b), bisLNA-m44a, with an additional LNA substitution (opposite

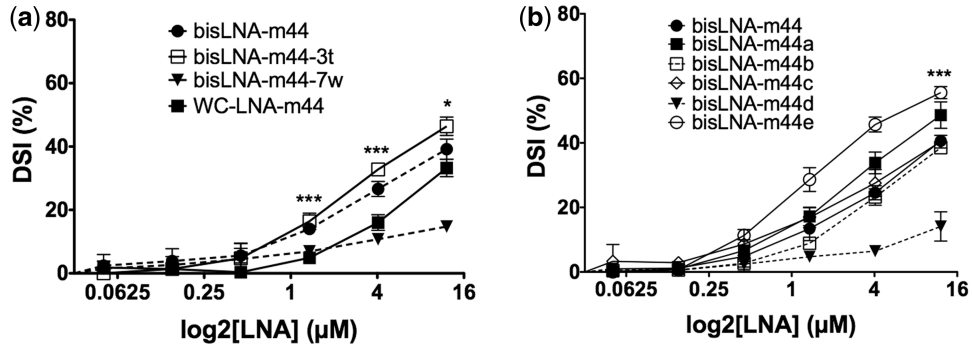

Figure 4. DSI efficiency comparison between different modified bisLNA-m44-derivatives. (**a**) Comparison between bisLNA-m44, bisLNA-m44-3t, bisLNA-m44-7w and WC-LNA-m44, having different TFO or Watson–Crick arm lengths. Hybridizations performed overnight at 37°C. Applying two-way ANOVA with Bonferroni posttest significant differences are found: bisLNA-m44 versus WC-LNA-m44 at 1.35 μM and 4.05 μM (***$P < 0.001$) and 12 μM (*$P < 0.05$). (**b**) Comparison between bisLNAs containing different LNA content and positioning as described in Table 3. LNAs were hybridized overnight at 37°C. ***$P < 0.001$ found for m44e versus m44 and m44e versus m44a at 12 μM (two-way ANOVA with Bonferroni posttest).

Table 3. LNA contents of the different bisLNAs

Construct	LNA positioning	LNA positioning (D = DNA; L = LNA)	LNA in Hoogsteen	LNA in Watson–Crick	LNA in tail	LNA total
bisLNA-m44a	Opposite	DLDLD / DLDLD	8	8	5	21
bisLNA-m44	Alternated	DLDLD / LDLDL	8	7	5	20
bisLNA-m44b	Alternated	See above	7	8	5	20
bisLNA-m44c	Opposite	See above	8	7	5	20
bisLNA-m44d	Opposite	See above	7	7	5	19
bisLNA-m44e	Alternated	See above	8	7	9	24

Schematic positioning of LNA bases are shown for the first two constructs, which exemplify the two possibilities (opposite or alternated positioning) with D representing a DNA base and L an LNA base.

LNAs 8TFO/8WC), was more efficient (49% at 12 μM) than the bisLNA-m44. There was no difference between the bisLNA-m44 and the bisLNA-m44b (alternated LNAs 7TFO/8WC) and bisLNA-m44c (opposite LNAs 8TFO/7WC) at the different concentrations. Surprisingly, the bisLNA-m44d (opposite LNAs 7TFO/7WC) showed poor strand invasion (12% at 12 μM), compared with all the other bisLNAs tail clamps. In contrast, the bisLNA-m44e, with a higher content of LNA in the tail, showed a significant increase ($P < 0.001$) of strand invasion (53% at 12 μM) compared with bisLNA-m44 and bisLNA-m44a and was efficient at lower concentration (24% at 1.35 μM).

BisLNA binding to a single site is able to withstand linearization of plasmid DNA

As previously studied for the 10-mer bisLNAs, we tested the ability of the longer bisLNAs to withstand linearization (loss of supercoiling) of plasmid DNA, when bound to a single site. Thus, a single BS plasmid was hybridized with bisLNA and then digested by REs. After running an agarose mobility shift assay, a qualitative examination of the gel bands (Figure 5) showed that bisLNA-m44-3t and bisLNA-m44a seemed to have a better ability to remain bound after linearization as compared with bisLNA-m44. Although this assay is informative, it is important to point out that the agarose gel electrophoresis is a rather harsh

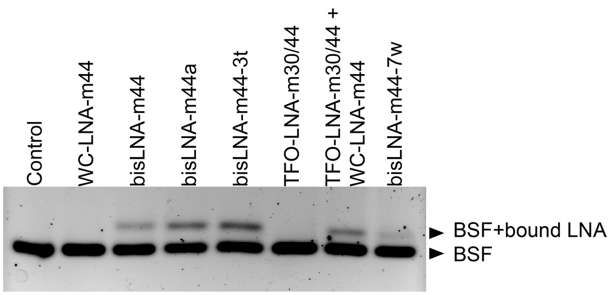

Figure 5. Agarose electrophoretic mobility shift assay showing the relative binding strength of different bisLNAs to binding site containing fragment (BSF) of pDel-1 after RE digestion-induced linearization of plasmid. Hybridization was performed overnight at 37°C.

assay for strand-invasion complexes, likely resulting in that a substantial fraction of the hybridized bisLNA falls off its linearized target DNA fragment during this procedure (56,57). Not surprisingly, bisLNA-m44-7w showed a comparatively weak, but yet, detectable band, confirming the poor strand-invasion capacity detected in the S1 assay. It is noteworthy that we could not detect any binding of WC-LNA-m44 or of TFO-LNA-m30/44 alone; however, when they were co-incubated with the plasmid, binding was detected. Taken together, these results clearly illustrate a superior ability of bisLNA to withstand linearization. It was also confirmed that the simultaneous addition of unlinked TFO- and WC arms provides binding synergy as previously demonstrated for the 10-mer bisLNAs.

Binding specificity to plasmid DNA

To test for specificity of our constructs, we used mutant plasmids, where we introduced single or double point mutations changing A bases in the target sequence into G or C, the latter disrupting the polypurine stretch used for TFO binding. The results in Figure 6a show a clear reduction of the DSI upon bisLNA-m44 binding to the mutant binding sites. When incubating pDel-1, containing the cognate BS, with 1.35 μM bisLNA-m44, a DSI of ~20% was reached after 72 h incubation, whereas ~9-fold higher concentration of ON was needed to reach the same level of DSI with the single-mutation plasmids. As expected, incubation with the double-mutant plasmids

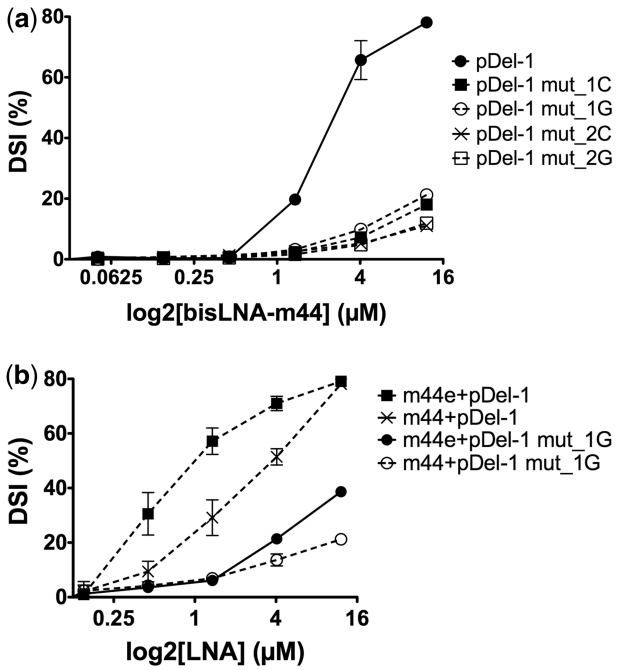

Figure 6. DSI efficiency for bisLNAs hybridized for 72 h at 37°C with pDel-1 and pDel-1-derived mutant plasmids. The mutant plasmids had either a single (mut_1) or double mutation (mut_2) on the target homopurine sequence. This mutation was either purine-to-purine (A→G) or purine-to-pyrimidine (A→C). (**a**) Hybridizations with bisLNA-m44. (**b**) Side by side comparison between hybridizations of pDel-1 and pDel-1 mut_1G (with an A→G mutation) with bisLNA-m44 and bisLNA-m44e.

further reduced the binding of bisLNA-m44 to a maximum of 12% binding efficiency at the highest concentration and with no significant differences between the two mutant plasmid constructs. Also bisLNA-m44e, having a higher percentage of LNA, was tested for specificity with plasmid pDel-1 mut_1G (which was giving the highest non-specific binding with construct bisLNA-m44), by performing incubations for 72 h (Figure 6b). Non-specific binding only exceeded that of bisLNA-m44 at concentrations above 1.35 μM. On the other hand, bisLNA-m44e reached a DSI efficiency of 30% already at 0.45 μM while bisLNA-m44 reached the same effect at a 4-fold higher concentration. Thus, while increasing the LNA content makes the construct less discriminatory, whether this behaviour represents an impediment also in a cellular context remains to be investigated.

Effect of the flanking region

The promoter region in the human *MYC* gene is interesting as a potential target for anti-gene strategies. However, previous studies (58–60) have demonstrated the presence of a highly structured region upstream the P1 promoter containing either a G-quadruplex or an H-DNA conformation at a distance of 11 bp from the bisLNA binding site. To rule out any possible influence of this structure on the bisLNA DSI when using the pDel-1 plasmids (as these plasmids contain the full length *MYC* promoter sequence), the bisLNA-binding site lacking the adjacent G-quartet sequence was introduced into the pEGFP-Luc plasmid (Supplementary Figure S6a). Using the same hybridization conditions, bisLNA-m44 showed comparable efficiency in terms of DSI in relation to all examined plasmids (Supplementary Figure S6b), suggesting that bisLNA-m44 is able to achieve DSI at sequences forming canonical B-DNA. We subsequently investigated whether the bisLNA can strand-invade into another site in the genomic *MYC* region, located downstream of the P1 promoter and known as the P2 promoter. By targeting this site in the Del-1 plasmid, with bisLNA-m(P2)37 we were also able to achieve strand-invasion (30% after overnight incubation and 70% after 3 days incubation at 12 μM). Importantly, for this construct DSI could be detected even at 50 and 150 nM (Figure 7 and Supplementary Figure S7). This result suggests that the bisLNA can be used for different homopurine stretch in the genome.

Thermal melting measurements

For technical reasons, T_m measurements (Table 4) were carried out with linear DNA fragments containing the target sequence, i.e. not under DSI conditions. Among the 10-mer bisLNAs, the most stable triplex was formed with the bisLNA-20. The experiments also re-enforced that LNA modifications stabilize the triplex more when they are located in the TFO arm (bisLNA-20a) than in the WC arm (bisLNA-20b), while the introduction of LNA nucleotides in both arms (bisLNA-20) provided, as expected, the highest triplex stability. Thermal melting curves for bisLNA-20 (Supplementary Figure S8) clearly show two melting transitions, the first one, at the lower

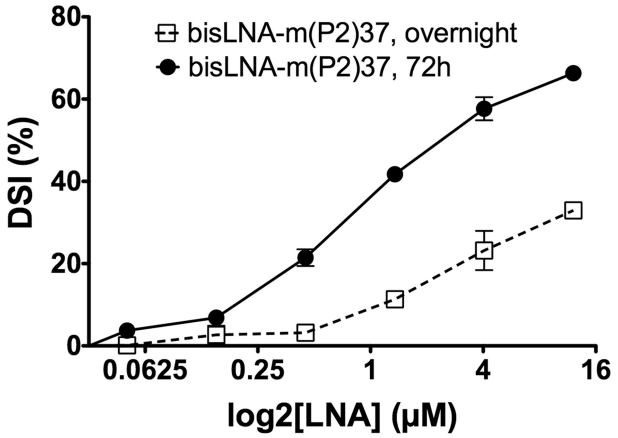

Figure 7. DSI efficiency for bisLNA-m(P2)37 hybridized overnight or for 72 h with pDel-1 (the cognate site being located at the P2 promoter region of the c-*MYC* gene).

Table 4. T_m values (°C) determined for the melting of the triplexes (as determined by UV spectroscopy—Supplementary Figure S8)

Construct	Hybridization condition	T_m (°C)
bisLNA-20	20 mM $NaPO_4$; pH 5.8	63
bisLNA-20a	20 mM $NaPO_4$; pH 5.8	40
bisLNA-20b	20 mM $NaPO_4$; pH 5.8	34
bisLNA-m30	20 mM $NaPO_4$; pH 7.3	66
WC-LNA-m30	20 mM $NaPO_4$; pH 7.3	48
bisLNA-m44	20 mM $NaPO_4$; pH 7.3	78
bisLNA-m44-3t	20 mM $NaPO_4$; pH 7.3	75
WC-LNA-m44	20 mM $NaPO_4$; pH 7.3	82
WC-LNA-m44 + TFO-LNA-m30/44	20 mM $NaPO_4$; pH 7.3	82

temperature, corresponding to the TFO dissociation and the second one to the Watson–Crick dissociation. This is not seen for the other 10-mer bisLNAs tested, which only presents the Watson–Crick dissociation, thus suggesting higher instability of the triplex domain.

Under the same conditions (20 mM phosphate pH 5.8), the thermal melting measurement were out of range for bisLNA-m30 and bisLNA-m44 owing to their longer sequences and their higher affinity. To measure their T_m, we performed the study at intracellular pH 7.3, and low salt conditions, which should decrease binding affinity, especially Hoogsteen binding. BisLNA-m30 and bisLNA-m44 were subsequently compared with their LNA WC arm counterparts (WC-LNA-m30 and WC-LNA-m44). For bisLNA-m30, we noticed a marked T_m increase ($\Delta = +18°C$) in comparison with its WC arm (WC-LNA-m30). Surprisingly, bisLNA-m44 showed no additional thermal stabilization by the TFO arm, with even a slight decrease in T_m ($\Delta = -4°C$) in comparison with its WC arm alone, nevertheless as stated before the experiments were conducted in low salt and pH 7.3, which make the triplex formation less stable. The same was true when comparing with the corresponding two separate arms (WC-LNA-m44 and TFO-LNA-m30/44). On the other hand, and as expected, bisLNA-m44 showed as a slightly higher T_m ($\Delta = +3°C$) when compared with bisLNA-m44-3t, which lacks three bases in the TFO arm.

Characterization of bisLNA and non-bisLNA binding to double-strand DNA

To further examine LNA ON binding to supercoiled double-strand DNA, we mapped the ss regions, resulting from binding of bisLNA or the corresponding LNA devoid of the TFO portion, using a chemical probing assay.

DNA chemical modification was performed using chloroacetaldehyde treatment (CAA) (61) of plasmid pEGFPLuc-bisBSf containing a DNA target sequence derived from the *MYC* promoter region. CAA reacts preferably with the exocyclic amino group of adenines and cytosines, which makes the DNA more susceptible to alkali cleavage at the reacted DNA sites (62). CAA-modified nucleotides were identified using each of the treated DNA strands as template in a primer-extension (PE) reaction using ^{32}P-labelled primers. Hybridization of bisLNA-m44 (12 μM, 78 h and 37°C) resulted in efficient DNA invasion and binding, in both the triplex- and Watson–Crick regions, which can be seen in Figure 8a (lane 4) as compared to controls in the absence of a DNA-binding ON (lanes 1 and 2). In addition, we introduced controls where the DNA plasmid was targeted with bisLNA-m44 or the corresponding version devoid of the TFO portion, WC-LNA-m44, under similar conditions and then used as templates in the PE reaction without prior CAA treatment (lanes 3 and 5, respectively). These controls are used to distinguish any bands that may arise from polymerase pausing caused by the presence of remaining bisLNA-m44 or WC-LNA-m44 in the PE reaction. The distinct bands corresponding to CAA base modifications of C, A, and to some extent G, of the pyrimidine-rich strand in the presence of bisLNA-m44 clearly demonstrates formation of an ss region (D-loop) indicating a DNA-invasion event (Figure 8a, lane 4). Furthermore, we were able to detect additional modified nucleotides (indicated as *) outside of the binding site, mainly, but not exclusively, in the 3′-flanking region. Moreover, CAA-base modification of the D-loop strand was also detected in DNA targeted with an LNA ON devoid of the TFO portion (WC-LNA-m44) under similar conditions (lane 6). However, the intensity of the corresponding bands is much higher in the presence of the bisLNA compared with an LNA devoid of the TFO region (lanes 4 and 6, respectively), indicating that an LNA–DNA complex is formed to a higher extent in the presence of the bisLNA (bisLNA-m44).

CAA-mediated chemical modification of DNA hybridized with bisLNA-m44 or WC-LNA-m44 was also used to examine formation of ss regions on the purine-rich (LNA-binding) strand. We detected CAA modifications at the 3′-end junction of the bisLNA-binding strand, indicating the presence of a short ss region (Figure 8b, lane 4). On the other hand, the corresponding bands were not visible in the case when DNA was targeted by WC-LNA-m44 (lane 6). Also, we detected several bands within the BS, which we believe are a consequence of polymerase pausing, as they were equally present in

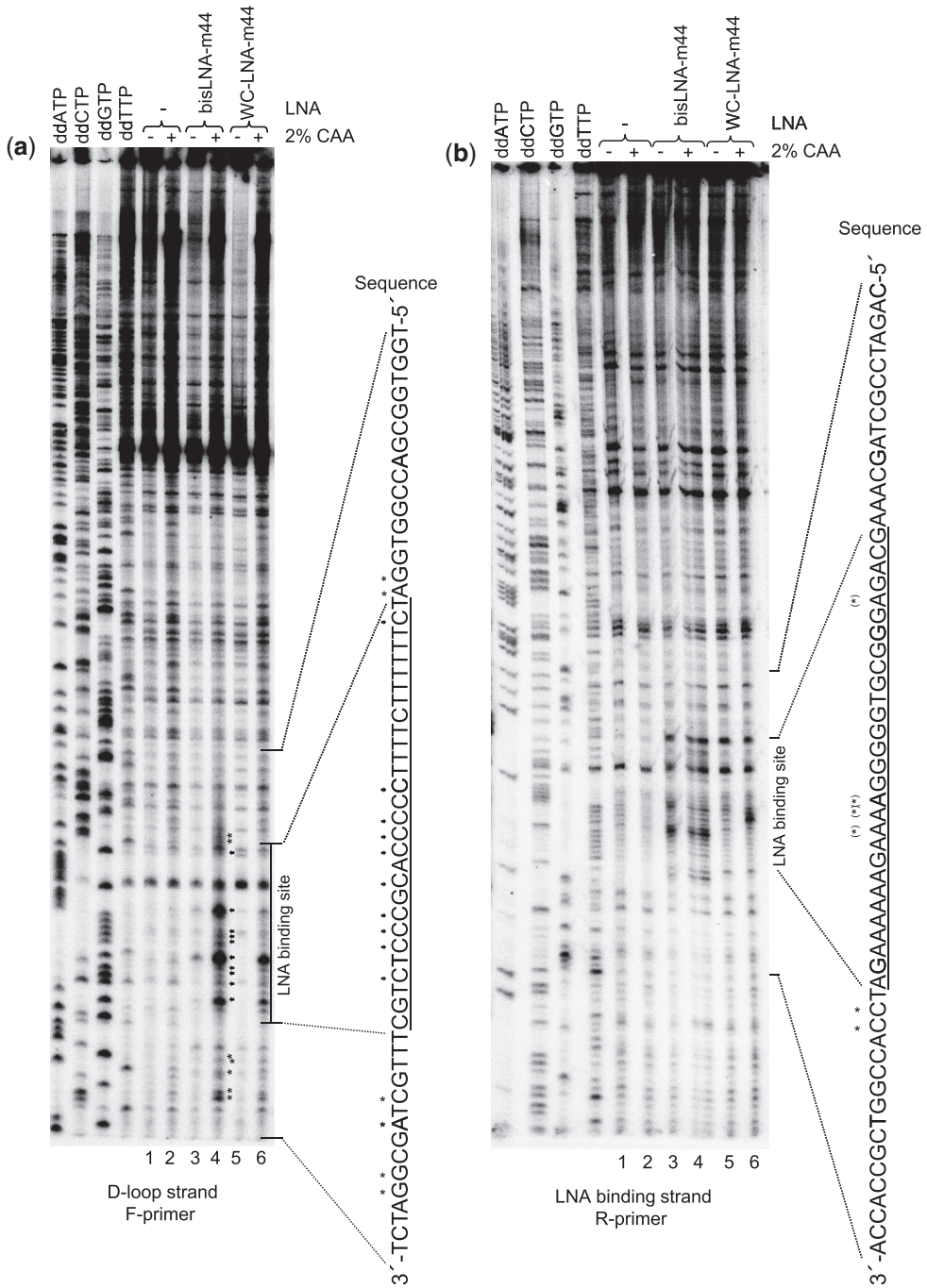

Figure 8. CAA base modification and analysis of bisLNA or LNA devoid of the TFO portion binding to pEGFPLuc-bisBSf using primer extension reaction and PAGE. (**a**) Analysis of the pyrimidine-rich strand (D-loop). Lanes 1 and 2: control plasmid, 3 and 4: plasmid hybridized with bisLNA-m44, and lanes 5 and 6: hybridized with WC-LNA-m44. Lanes 1, 3 and 5 are controls and lanes 2, 4 and 6 contain 2% CAA-treated plasmids. The DNA sequence complementary to the LNA binding-site (underlined) and flanking sequences are shown. CAA-modified nucleotides within the BS and in the flanking regions are indicated with ← or with *. (**b**) Analysis of the LNA-binding, purine-rich strand. Lanes 1 and 2: control plasmid, 3 and 4 (lane 4 appears as a split lane): plasmid hybridized with bisLNA-m44 and lanes 5 and 6: hybridized with WC-LNA-m44. Lanes 1, 3 and 5 are controls and lanes 2, 4 and 6 contains 2% CAA-treated plasmids. DNA sequence of the LNA-binding site (underlined) and flanking regions are shown. CAA-modified nucleotides are indicated. CAA base modifications were made on linearized plasmid.

CAA-treated and non-treated samples in the presence of bisLNA, as shown in Figure 8b (lanes 3 and 4, respectively). However, a different pattern of bands within the BS is observed in the presence of WC-LNA-m44, which may represent CAA modifications at the 5′-stretch of adenosines as shown in lane 6 [indicated as (*)].

DISCUSSION

In this report, we have investigated LNA-based clamp-type ONs and optimized them for targeting of dsDNA under physiological conditions. To our knowledge, this is the first study clearly showing the advantageous

influence of LNA bases in the design of a clamp-type ON (the bisLNA) to achieve combined triplex binding and duplex invasion. In the study of Hertoghs *et al*., from 2003 (43), a short 9-mer bisLNA was tested and found inferior as compared with linear LNAs. This was despite hybridizations at the non-physiological pH of 5.8, favouring binding of cytosine-containing TFOs. We have found that optimally designed bisLNAs efficiently strand-invade into supercoiled duplex DNA also under physiological pH and intranuclear ion concentration conditions.

There is already a vast literature on the behaviour of bis-type constructs using PNA-building blocks. Although this concept has been highly successful, especially under low-salt conditions, where the uncharged backbone of PNA is advantageous, there are also limitations. Thus, as reviewed by Nielsen (15), the on-rates for bis-PNA complexes are particularly slow under physiologically relevant conditions in buffers containing intracellular K^+ and Mg^{2+} concentrations, potentially severely compromising cellular and *in vivo* applications. However, as also stated in this review, biological processes, such as naturally occurring negative supercoiling, found in bacterial plasmids, or RNA:DNA hybrids, known as R-loops, observed in both prokaryotic and eukaryotic DNA under active transcription, may compensate for the slow on-rate by significantly increasing helix dynamics. Thus, DNA breathing (63,64) is enhanced by the tension induced by negative supercoiling (65). Moreover, in this process the DNA strand not bound in the R-loop is released from the duplex, thereby promoting its hybridization. It was recently reported that R-loop-forming sequences are found in the majority of human genes (66) and, as reviewed by Aguilera and Garcia-Muse (67), accumulating evidence suggests that R-loops form more frequently than previously anticipated.

Of importance for the interpretation of the data on bisLNAs in this report is the fact that, apart from the initial studies with the short 10-mer bisLNAs, all other experiments were carried out under intranuclear pH and ion concentration conditions. Given that this is the first study of the bisLNA concept, we aim at future improvements in both design and composition to enable efficient binding to chromosomal DNA. As an example, we have recently shown that replacing LNA with N2′-glycyl-2′-amino-LNA enhances Zorro-LNA-mediated DSI (20). It will be interesting to see what effect such substitutions will have for bisLNAs.

In the initial studies using the 10-mer bis-oligonucleotide (bisON), we demonstrate the advantages of substituting DNA for LNA in both the TFO domain (TFO arm) and the duplex-forming domain (Watson–Crick arm). The LNA substitution was chosen to be 50%, as it was already known that a fully LNA-substituted TFO is binding with less efficiency, likely reflecting the extreme rigidity imparted by the locked C3′-endo configuration of the LNAs (31,68). Linking both TFO- and WC-binding domains generated much stronger binding, which could even withstand linearization of the supercoiled DNA. This is in contrast to mixed DNA/LNA single-stranded ONs that have been shown, in previous reports (50) and our present one, not to be able to remain bound to linear dsDNA. The results obtained with the use of the non-linked domains suggest that the increased binding/duplex invasion is possibly not only due to the local increase of concentration when TFO and Watson-Crick arms are linked together, but could also be attributed to local conformation changes on the target DNA strand imparted by the LNA-modified TFO or duplex-binding domains. LNA–DNA duplexes have been shown previously to attain a structure similar to an A-type helix, conveyed by the N-type conformation of LNA monomers (69–73). The change in conformation from S-type to N-type induced by the LNA monomers is responsible for pre-organizing single-stranded LNA oligomers, thereby influencing the duplex formation with DNA resulting in the increased affinity (30). Similarly, an LNA-based TFO seems also to prefer an A-type of helix. Thus, it was previously demonstrated that LNA is suitable for the pyrimidine motif triple helix (31) and that the DNA duplex of a triple helix, formed by an LNA-containing TFO, adopted an overall intermediate structure between A- and B-type, in order to accommodate the LNA strand (68).

The UV melting assay revealed several aspects of bisLNA triplex formation. The dissociation and association of bisLNAs was investigated by using heating or cooling steps. The most interesting effect observed was the increase of T_m induced by TFO-arm binding. In the particular case of bisLNA-m30, the derivatives for the association and the dissociation curves showed significant hysteresis. This could arise owing to the thermodynamic equilibrium between the melting curves not being reached, indicating slow steps in the association and /or dissociation reactions, which could not be overcome even for a slow ramp rate of 0.2°C/min. This phenomenon is actually not observed for the other bisLNA constructs tested, which could be attributed to significantly faster rates of triplex formation (74,75). Another conclusion from the melting study was that the presence of LNA in both arms is a stabilizing factor for the triplex. For that, we have compared the melting properties for bisLNA-20, with the LNA-m20a and LNA-m20b. This result is consistent with the results of GEFA (Supplementary Figure S4) and S1 assay (Supplementary Figure S3), showing that the bisLNA-20 was the best construct owing to the presence of LNAs in both arms.

When constructing the bisLNA, we found that it was optimal to have the linker region composed of five to six DNA bases instead of non-natural linkers. Five were used in all construct with the exception of the bisLNA-m(P2)37, where six nucleotides were introduced. A strict comparison between 5- and 6-nucleotide linkers was never carried out, but both provided efficient invasion. This goes in line with previous findings, where a natural nucleotide linker in the context of a full DNA-based triplex has been shown to have positive characteristics, such as favourable stacking interactions involving the loop bases and the possibility to establish stabilizing base-pairing interactions between the first/last loop bases and the base adjacent to the minimal BS (47,76). Thus, our results obtained with a triplex-forming bisLNA seem to follow the same

pattern as observed for a DNA-based triplex in these earlier studies.

The sequence used by us has a low percentage of cytosine bases in the TFO sequence, which would in principle render it less pH dependent. At the same time, LNA-C bases are methylated, which also improves the Hoogsteen binding at physiological pH (77). Moreover, binding at physiological conditions is certainly not only enhanced due to the stabilization effect of the LNA-bases (16), but also, likely because of the contribution of the bisLNA mode of binding.

Our findings show that bisLNA binding to dsDNA is highly efficient (80% after 72 h). It should also be noted that all plasmid preparations always contain nicked plasmids, which are not suitable targets for bisLNA DSI, and no efforts were made here to examine different experimental conditions to reach 100% binding. We believe that *in vivo* even longer exposure times are physiologically relevant, as many tissues cells are non-dividing over long periods of time and LNA/DNA mixmer ONs may exert effects for days or even weeks.

An interesting aspect is that the tail-clamp bisLNA-m44 showed a decent discrimination against a site with a single mutation. At the highest concentration tested (12 μM), the DSI was ~18 and 21% for bisLNA-m44 incubated for 3 days with plasmid containing one purine (A) to purine (G) mutation or purine (A) to pyrimidine (C) mutation, respectively. However, for its cognate site, bisLNA-m44 reached ~20% binding at 9× lower concentration (1.35 μM). A further increase in the LNA content on bisLNA-m44e led to both an increased DSI efficiency (~4-fold at an intermediate concentration of 1.35 μM) and increased non-specific binding albeit only at the highest concentrations tested (4.05 and 12 μM) when comparing with bisLNA-m44. Although an increase in non-specific binding should be avoided, it is also true that the specificity tests used here are giving us a simplistic model. Thus, it is hard to extrapolate to possible effects in the context of a cell.

We also investigated the possibility to reduce the length of both the 'tail' and the TFO separately. While maintaining the TFO length, shortening of the tail decreases the efficiency for DSI. It is therefore likely that the bisLNA tail is crucial for efficient strand-invasion, which is also consistent with the poor DSI for bisLNA-30 lacking the 'tail'. On the contrary, shortening of the TFO arm (by only three bases) instead marginally increased the DSI capacity. It is noticed that WC-LNA-m44 (WC arm alone) is able to strand-invade without the help of the TFO arm. However, WC-LNA-m44 performs DSI with a significantly lower efficiency and more importantly, it is completely 'kicked-out' when the super-coiling is lost (e.g. owing to plasmid linearization by enzymatic digestion), while a tail-clamp bisLNA remains bound. In a cellular context where genomic DNA can, by virtue of DNA/RNA polymerase action, unwind, it is crucial that bisLNA binding can resist this conformational change.

Undoubtedly our results point in the direction that an optimized design is necessary to exploit the full bisLNA potential for DSI and possible gene blocking capacity. We thought that a further improvement on the bisLNA design could result from the LNA-base positioning. A comparison between LNAs m44b, m44 and m44c showed the same efficiency in terms of DSI with the same total number of LNA residues regardless of their positioning. However, with bisLNA-m44a and bisLNA-m44d, we did get different DSI capacities when comparing with e.g. bisLNA-m44. A reason could be the total number of LNA nucleotides (one more LNA for m44a and one less LNA for m44d). Alternatively, it can be caused by the proximity of the LNA nucleotides to the linker (very close for the bisLNA-m44a, more separated for bisLNA-m44d and intermediate for LNAs m44b, m44 and m44c).

We have also demonstrated the ability of the bisLNA to DSI independently of the flanking region by targeting two different sites in the *MYC* promoter region and introducing the BS into a different plasmid and in different orientations. Thus, any polypurine–polypyrimidine site is a potential target, and this result opens the possibility for a large spectrum of applications for bisLNAs. Furthermore, we have shown that plasmid DNA targeting by bisLNA or by a non–TFO-containing LNA ON results in DSI and formation of a D-loop. Chemical probing using CAA base modification enabled us to map the site of formation of the single-strand region with one nucleotide resolution. Our results demonstrate that bisLNA (bisLNA-m44) is more efficient in targeting duplex DNA than the corresponding LNA devoid of a TFO arm (WC-LNA-m44) (Figure 8a). Also, we observed few bands indicating possible CAA modification within the DNA target site of the WC-LNA-m44, which suggests that a less stable LNA–DNA complex is formed in the presence of WC-LNA-m44 (Figure 8b).

DSI represents a major challenge for synthetic ONs though several highly interesting studies demonstrating anti-gene effects of non–triplex-forming ONs based on PNA or LNA chemistry exist (28,78–80). However, direct evidence for DSI is frequently lacking, and, to the best of our knowledge, until now PNA is the chemistry for which there has been the strongest evidence for robust DSI.

In conclusion, increasing the target sequence from 10 to 15 bases made it possible to achieve robust DSI under intranuclear ion concentration and pH conditions. Compared with the first used regular bisLNA-m30, adding the tail in the bisLNA-m44 tail-clamp construct enhanced DSI 25-fold, and increasing the LNA content in the tail caused a further improvement by a factor of 4. This means that we have already achieved a 100-fold increase in potency by combining changes of the design and in the LNA content of the bisLNA. Moreover, using this enhanced bisLNA, 30% DSI was obtained at a concentration of 450 nM, corresponding to a bisLNA:plasmid ratio of only 21:1 (Figure 6b). This is highly promising for future *in vivo* studies, as in each cell there are only one or two target sites, one on each chromosome, and we expect to be able to achieve significantly higher ratios when treating cells.

SUPPLEMENTARY DATA

Supplementary Data are available at NAR Online: Supplementary Figures 1–8.

FUNDING

Swedish Research Council; Swedish Cancer Society; EU FP7 [CHAARM grant no. 242135]; 'European Innovative Research & Technological Development Projects in Nanomedicine' within the framework of the ERA-NET EuroNanoMed; Danish National Research Foundation for funding the Nucleic Acid Center; Portuguese Foundation for Science and Technology (FCT) [Ph.D grant SFRH/BD/16757/2004] (to P.M.); EU-FP7-PEOPLE-ITN-2008 [PhosChemRec grant no. 238579] (to S.G. and C.S.J.R.). Funding for open access charge: Swedish Research Council.

Conflict of interest statement. None declared.

REFERENCES

1. Bennett,C.F. and Swayze,E.E. (2010) RNA targeting therapeutics: molecular mechanisms of antisense oligonucleotides as a therapeutic platform. *Annu. Rev. Pharmacol. Toxicol.*, **50**, 259–293.
2. Moser,H.E. and Dervan,P.B. (1987) Sequence-specific cleavage of double helical DNA by triple helix formation. *Science*, **238**, 645–650.
3. Le Doan,T., Perrouault,L., Praseuth,D., Habhoub,N., Decout,J.L., Thuong,N.T., Lhomme,J. and Helene,C. (1987) Sequence-specific recognition, photocrosslinking and cleavage of the DNA double helix by an oligo-[alpha]-thymidylate covalently linked to an azidoproflavine derivative. *Nucleic Acids Res.*, **15**, 7749–7760.
4. Young,S.L., Krawczyk,S.H., Matteucci,M.D. and Toole,J.J. (1991) Triple helix formation inhibits transcription elongation in vitro. *Proc. Natl. Acad. Sci. USA*, **88**, 10023–10026.
5. Kim,H.G. and Miller,D.M. (1995) Inhibition of in vitro transcription by a triplex-forming oligonucleotide targeted to human c-myc P2 promoter. *Biochemistry*, **34**, 8165–8171.
6. McGuffie,E.M. and Catapano,C.V. (2002) Design of a novel triple helix-forming oligodeoxyribonucleotide directed to the major promoter of the c-myc gene. *Nucleic Acids Res.*, **30**, 2701–2709.
7. Ebbinghaus,S.W., Fortinberry,H. and Gamper,H.B. Jr (1999) Inhibition of transcription elongation in the HER-2/neu coding sequence by triplex-directed covalent modification of the template strand. *Biochemistry*, **38**, 619–628.
8. Faria,M., Wood,C.D., Perrouault,L., Nelson,J.S., Winter,A., White,M.R., Helene,C. and Giovannangeli,C. (2000) Targeted inhibition of transcription elongation in cells mediated by triplex-forming oligonucleotides. *Proc. Natl. Acad. Sci. USA*, **97**, 3862–3867.
9. Kuznetsova,S., Ait-Si-Ali,S., Nagibneva,I., Troalen,F., Le Villain,J.P., Harel-Bellan,A. and Svinarchuk,F. (1999) Gene activation by triplex-forming oligonucleotide coupled to the activating domain of protein VP16. *Nucleic Acids Res.*, **27**, 3995–4000.
10. Xu,X.S., Glazer,P.M. and Wang,G. (2000) Activation of human gamma-globin gene expression via triplex-forming oligonucleotide (TFO)-directed mutations in the gamma-globin gene 5′ flanking region. *Gene*, **242**, 219–228.
11. Wang,G., Levy,D.D., Seidman,M.M. and Glazer,P.M. (1995) Targeted mutagenesis in mammalian cells mediated by intracellular triple helix formation. *Mol. Cell. Biol.*, **15**, 1759–1768.
12. Kalish,J.M., Seidman,M.M., Weeks,D.L. and Glazer,P.M. (2005) Triplex-induced recombination and repair in the pyrimidine motif. *Nucleic Acids Res.*, **33**, 3492–3502.
13. Puri,N., Majumdar,A., Cuenoud,B., Natt,F., Martin,P., Boyd,A., Miller,P.S. and Seidman,M.M. (2001) Targeted gene knockout by 2′-O-aminoethyl modified triplex forming oligonucleotides. *J. Biol. Chem.*, **276**, 28991–28998.
14. Cassidy,R.A., Puri,N. and Miller,P.S. (2003) Effect of DNA target sequence on triplex formation by oligo-2′-deoxy- and 2′-O-methylribonucleotides. *Nucleic Acids Res.*, **31**, 4099–4108.
15. Nielsen,P.E. (2010) Gene targeting and expression modulation by peptide nucleic acids (PNA). *Curr. Pharm. Des.*, **16**, 3118–3123.
16. Sun,B.W., Babu,B.R., Sorensen,M.D., Zakrzewska,K., Wengel,J. and Sun,J.S. (2004) Sequence and pH effects of LNA-containing triple helix-forming oligonucleotides: physical chemistry, biochemistry, and modeling studies. *Biochemistry*, **43**, 4160–4169.
17. Brunet,E., Alberti,P., Perrouault,L., Babu,R., Wengel,J. and Giovannangeli,C. (2005) Exploring cellular activity of locked nucleic acid-modified triplex-forming oligonucleotides and defining its molecular basis. *J. Biol. Chem.*, **280**, 20076–20085.
18. Brunet,E., Corgnali,M., Cannata,F., Perrouault,L. and Giovannangeli,C. (2006) Targeting chromosomal sites with locked nucleic acid-modified triplex-forming oligonucleotides: study of efficiency dependence on DNA nuclear environment. *Nucleic Acids Res.*, **34**, 4546–4553.
19. Ge,R., Heinonen,J.E., Svahn,M.G., Mohamed,A.J., Lundin,K.E. and Smith,C.I. (2007) Zorro locked nucleic acid induces sequence-specific gene silencing. *FASEB J.*, **21**, 1902–1914.
20. Zaghloul,E.M., Madsen,A.S., Moreno,P.M., Oprea,II., El-Andaloussi,S., Bestas,B., Gupta,P., Pedersen,E.B., Lundin,K.E., Wengel,J. *et al.* (2011) Optimizing anti-gene oligonucleotide 'Zorro-LNA' for improved strand invasion into duplex DNA. *Nucleic Acids Res.*, **39**, 1142–1154.
21. Goni,J.R., de la Cruz,X. and Orozco,M. (2004) Triplex-forming oligonucleotide target sequences in the human genome. *Nucleic Acids Res.*, **32**, 354–360.
22. Goni,J.R., Vaquerizas,J.M., Dopazo,J. and Orozco,M. (2006) Exploring the reasons for the large density of triplex-forming oligonucleotide target sequences in the human regulatory regions. *BMC Genomics*, **7**, 63.
23. Behe,M.J. (1995) An overabundance of long oligopurine tracts occurs in the genome of simple and complex eukaryotes. *Nucleic Acids Res.*, **23**, 689–695.
24. Mirkin,S.M., Lyamichev,V.I., Drushlyak,K.N., Dobrynin,V.N., Filippov,S.A. and Frank-Kamenetskii,M.D. (1987) DNA H form requires a homopurine-homopyrimidine mirror repeat. *Nature*, **330**, 495–497.
25. Htun,H. and Dahlberg,J.E. (1988) Single strands, triple strands, and kinks in H-DNA. *Science*, **241**, 1791–1796.
26. Boffa,L.C., Morris,P.L., Carpaneto,E.M., Louissaint,M. and Allfrey,V.G. (1996) Invasion of the CAG triplet repeats by a complementary peptide nucleic acid inhibits transcription of the androgen receptor and TATA-binding protein genes and correlates with refolding of an active nucleosome containing a unique AR gene sequence. *J. Biol. Chem.*, **271**, 13228–13233.
27. Hu,J. and Corey,D.R. (2007) Inhibiting gene expression with peptide nucleic acid (PNA)-peptide conjugates that target chromosomal DNA. *Biochemistry*, **46**, 7581–7589.
28. Beane,R., Gabillet,S., Montaillier,C., Arar,K. and Corey,D.R. (2008) Recognition of chromosomal DNA inside cells by locked nucleic acids. *Biochemistry*, **47**, 13147–13149.
29. Bentin,T., Larsen,H.J. and Nielsen,P.E. (2003) Combined triplex/duplex invasion of double-stranded DNA by "tail-clamp" peptide nucleic acid. *Biochemistry*, **42**, 13987–13995.
30. Petersen,M., Nielsen,C.B., Nielsen,K.E., Jensen,G.A., Bondensgaard,K., Singh,S.K., Rajwanshi,V.K., Koshkin,A.A., Dahl,B.M., Wengel,J. *et al.* (2000) The conformations of locked nucleic acids (LNA). *J. Mol. Recognit.*, **13**, 44–53.
31. Obika,S., Uneda,T., Sugimoto,T., Nanbu,D., Minami,T., Doi,T. and Imanishi,T. (2001) 2′-O,4′-C-Methylene bridged nucleic acid (2′,4′-BNA): synthesis and triplex-forming properties. *Bioorg. Med. Chem.*, **9**, 1001–1011.
32. Brunet,E., Alberti,P., Perrouault,L., Babu,R., Wengel,J. and Giovannangeli,C. (2005) Exploring cellular activity of locked nucleic acid-modified triplex-forming oligonucleotides and defining its molecular basis. *J. Biol. Chem.*, **280**, 20076–20085.
33. Torigoe,H., Hari,Y., Sekiguchi,M., Obika,S. and Imanishi,T. (2001) 2′-O,4′-C-methylene bridged nucleic acid modification promotes pyrimidine motif triplex DNA formation at physiological pH: thermodynamic and kinetic studies. *J. Biol. Chem.*, **276**, 2354–2360.
34. Xodo,L.E., Manzini,G. and Quadrifoglio,F. (1990) Spectroscopic and calorimetric investigation on the DNA triplex formed by d(C

TCTTCTTTCTTTTCTTTCTTCTC) and d(GAGAAGAAAGA) at acidic pH. *Nucleic Acids Res.*, **18**, 3557–3564.
35. Mergny,J.L., Sun,J.S., Rougee,M., Montenay-Garestier,T., Barcelo,F., Chomilier,J. and Helene,C. (1991) Sequence specificity in triple-helix formation: experimental and theoretical studies of the effect of mismatches on triplex stability. *Biochemistry*, **30**, 9791–9798.
36. Kandimalla,E.R. and Agrawal,S. (1994) Single-strand-targeted triplex formation: stability, specificity and RNase H activation properties. *Gene*, **149**, 115–121.
37. Egholm,M., Christensen,L., Dueholm,K.L., Buchardt,O., Coull,J. and Nielsen,P.E. (1995) Efficient pH-independent sequence-specific DNA binding by pseudoisocytosine-containing bis-PNA. *Nucleic Acids Res.*, **23**, 217–222.
38. Lundin,K.E., Good,L., Stromberg,R., Graslund,A. and Smith,C.I. (2006) Biological activity and biotechnological aspects of peptide nucleic acid. *Adv. Genet.*, **56**, 1–51.
39. Demidov,V.V., Yavnilovich,M.V., Belotserkovskii,B.P., Frank-Kamenetskii,M.D. and Nielsen,P.E. (1995) Kinetics and mechanism of polyamide ("peptide") nucleic acid binding to duplex DNA. *Proc. Natl. Acad. Sci. USA*, **92**, 2637–2641.
40. Kuhn,H., Demidov,V.V., Nielsen,P.E. and Frank-Kamenetskii,M.D. (1999) An experimental study of mechanism and specificity of peptide nucleic acid (PNA) binding to duplex DNA. *J. Mol. Biol.*, **286**, 1337–1345.
41. Kaihatsu,K., Shah,R.H., Zhao,X. and Corey,D.R. (2003) Extending recognition by peptide nucleic acids (PNAs): binding to duplex DNA and inhibition of transcription by tail-clamp PNA-peptide conjugates. *Biochemistry*, **42**, 13996–14003.
42. Bentin,T., Hansen,G.I. and Nielsen,P.E. (2006) Structural diversity of target-specific homopyrimidine peptide nucleic acid-dsDNA complexes. *Nucleic Acids Res.*, **34**, 5790–5799.
43. Hertoghs,K.M., Ellis,J.H. and Catchpole,I.R. (2003) Use of locked nucleic acid oligonucleotides to add functionality to plasmid DNA. *Nucleic Acids Res.*, **31**, 5817–5830.
44. Lundin,K.E., Ge,R., Svahn,M.G., Tornquist,E., Leijon,M., Branden,L.J. and Smith,C.I. (2004) Cooperative strand invasion of supercoiled plasmid DNA by mixed linear PNA and PNA-peptide chimeras. *Biomol. Eng.*, **21**, 51–59.
45. He,T.C., Sparks,A.B., Rago,C., Hermeking,H., Zawel,L., da Costa,L.T., Morin,P.J., Vogelstein,B. and Kinzler,K.W. (1998) Identification of c-MYC as a target of the APC pathway. *Science*, **281**, 1509–1512.
46. Prakash,G. and Kool,E.T. (1992) Structural effects in the recognition of DNA by circular oligonucleotides. *J. Am. Chem. Soc.*, **114**, 3523–3527.
47. Rumney,S. and Kool,E.T. (1995) Structural optimization of non-nucleotide loop replacements for duplex and triplex DNAs. *J. Am. Chem. Soc.*, **117**, 5635–5646.
48. LaPlanche,L.A., James,T.L., Powell,C., Wilson,W.D., Uznanski,B., Stec,W.J., Summers,M.F. and Zon,G. (1986) Phosphorothioate-modified oligodeoxyribonucleotides. III. NMR and UV spectroscopic studies of the Rp-Rp, Sp-Sp, and Rp-Sp duplexes, [d(GGSAATTCC)]2, derived from diastereomeric O-ethyl phosphorothioates. *Nucleic Acids Res.*, **14**, 9081–9093.
49. Hacia,J.G., Wold,B.J. and Dervan,P.B. (1994) Phosphorothioate oligonucleotide-directed triple helix formation. *Biochemistry*, **33**, 5367–5369.
50. Lundin,K.E., Hasan,M., Moreno,P.M., Tornquist,E., Oprea,I., Svahn,M.G., Simonson,E.O. and Smith,C.I. (2005) Increased stability and specificity through combined hybridization of peptide nucleic acid (PNA) and locked nucleic acid (LNA) to supercoiled plasmids for PNA-anchored ''Bioplex'' formation. *Biomol. Eng.*, **22**, 185–192.
51. Roberts,J., Palma,E., Sazani,P., Orum,H., Cho,M. and Kole,R. (2006) Efficient and persistent splice switching by systemically delivered LNA oligonucleotides in mice. *Mol. Ther.*, **14**, 471–475.
52. Zhang,Y., Qu,Z., Kim,S., Shi,V., Liao,B., Kraft,P., Bandaru,R., Wu,Y., Greenberger,L.M. and Horak,I.D. (2011) Down-modulation of cancer targets using locked nucleic acid (LNA)-based antisense oligonucleotides without transfection. *Gene Ther.*, **18**, 326–333.
53. Hansen,J.B., Fisker,N., Westergaard,M., Kjaerulff,L.S., Hansen,H.F., Thrue,C.A., Rosenbohm,C., Wissenbach,M., Orum,H. and Koch,T. (2008) SPC3042: a proapoptotic survivin inhibitor. *Mol. Cancer Ther.*, **7**, 2736–2745.
54. Gupta,N., Fisker,N., Asselin,M.C., Lindholm,M., Rosenbohm,C., Orum,H., Elmen,J., Seidah,N.G. and Straarup,E.M. (2010) A locked nucleic acid antisense oligonucleotide (LNA) silences PCSK9 and enhances LDLR expression in vitro and in vivo. *PLoS One*, **5**, e10682.
55. Stein,C.A., Hansen,J.B., Lai,J., Wu,S., Voskresenskiy,A., Hog,A., Worm,J., Hedtjarn,M., Souleimanian,N., Miller,P. *et al.* (2010) Efficient gene silencing by delivery of locked nucleic acid antisense oligonucleotides, unassisted by transfection reagents. *Nucleic Acids Res.*, **38**, e3.
56. Rapireddy,S., He,G., Roy,S., Armitage,B.A. and Ly,D.H. (2007) Strand invasion of mixed-sequence B-DNA by acridine-linked, gamma-peptide nucleic acid (gamma-PNA). *J. Am. Chem. Soc.*, **129**, 15596–15600.
57. Chenna,V., Rapireddy,S., Sahu,B., Ausin,C., Pedroso,E. and Ly,D.H. (2008) A simple cytosine to G-clamp nucleobase substitution enables chiral gamma-PNAs to invade mixed-sequence double-helical B-form DNA. *ChemBioChem*, **9**, 2388–2391.
58. Yang,D. and Hurley,L.H. (2006) Structure of the biologically relevant G-quadruplex in the c-MYC promoter. *Nucleosides Nucleotides Nucleic Acids*, **25**, 951–968.
59. Belotserkovskii,B.P., De Silva,E., Tornaletti,S., Wang,G., Vasquez,K.M. and Hanawalt,P.C. (2007) A triplex-forming sequence from the human c-MYC promoter interferes with DNA transcription. *J. Biol. Chem.*, **282**, 32433–32441.
60. Wang,G. and Vasquez,K.M. (2004) Naturally occurring H-DNA-forming sequences are mutagenic in mammalian cells. *Proc. Natl. Acad. Sci. USA*, **101**, 13448–13453.
61. Kusmierek,J.T. and Singer,B. (1982) Chloroacetaldehyde-treated ribo- and deoxyribopolynucleotides. 1. Reaction products. *Biochemistry*, **21**, 5717–5722.
62. Kohwi-Shigematsu,T. and Kohwi,Y. (1992) Detection of non-B-DNA structures at specific sites in supercoiled plasmid DNA and chromatin with haloacetaldehyde and diethyl pyrocarbonate. *Methods Enzymol.*, **212**, 155–180.
63. Gueron,M., Kochoyan,M. and Leroy,J.L. (1987) A single mode of DNA base-pair opening drives imino proton exchange. *Nature*, **328**, 89–92.
64. Krueger,A., Protozanova,E. and Frank-Kamenetskii,M.D. (2006) Sequence-dependent base pair opening in DNA double helix. *Biophys. J.*, **90**, 3091–3099.
65. Liu,L.F. and Wang,J.C. (1987) Supercoiling of the DNA template during transcription. *Proc. Natl. Acad. Sci. USA*, **84**, 7024–7027.
66. Wongsurawat,T., Jenjaroenpun,P., Kwoh,C.K. and Kuznetsov,V. (2013) Quantitative model of R-loop forming structures reveals a novel level of RNA-DNA interactome complexity. *Nucleic Acids Res.*, **40**, e16.
67. Aguilera,A. and Garcia-Muse,T. (2012) R loops: from transcription byproducts to threats to genome stability. *Mol. Cell*, **46**, 115–124.
68. Sorensen,J.J., Nielsen,J.T. and Petersen,M. (2004) Solution structure of a dsDNA:LNA triplex. *Nucleic Acids Res.*, **32**, 6078–6085.
69. Nielsen,C.B., Singh,S.K., Wengel,J. and Jacobsen,J.P. (1999) The solution structure of a locked nucleic acid (LNA) hybridized to DNA. *J. Biomol. Struct. Dyn.*, **17**, 175–191.
70. Nielsen,K.E., Singh,S.K., Wengel,J. and Jacobsen,J.P. (2000) Solution structure of an LNA hybridized to DNA: NMR study of the d(CT(L)GCT(L)T(L)CT(L)GC):d(GCAGAAGCAG) duplex containing four locked nucleotides. *Bioconjug. Chem.*, **11**, 228–238.
71. Nielsen,K.E., Rasmussen,J., Kumar,R., Wengel,J., Jacobsen,J.P. and Petersen,M. (2004) NMR studies of fully modified locked nucleic acid (LNA) hybrids: solution structure of an LNA:RNA hybrid and characterization of an LNA:DNA hybrid. *Bioconjug. Chem.*, **15**, 449–457.
72. Ivanova,A. and Rosch,N. (2007) The structure of LNA:DNA hybrids from molecular dynamics simulations: the effect of locked nucleotides. *J. Phys. Chem. A*, **111**, 9307–9319.

73. Kaur,H., Arora,A., Wengel,J. and Maiti,S. (2006) Thermodynamic, counterion, and hydration effects for the incorporation of locked nucleic acid nucleotides into DNA duplexes. *Biochemistry*, **45**, 7347–7355.
74. Osborne,S.D., Powers,V.E., Rusling,D.A., Lack,O., Fox,K.R. and Brown,T. (2004) Selectivity and affinity of triplex-forming oligonucleotides containing 2′-aminoethoxy-5-(3-aminoprop-1-ynyl)uridine for recognizing AT base pairs in duplex DNA. *Nucleic Acids Res.*, **32**, 4439–4447.
75. Rusling,D.A., Powers,V.E., Ranasinghe,R.T., Wang,Y., Osborne,S.D., Brown,T. and Fox,K.R. (2005) Four base recognition by triplex-forming oligonucleotides at physiological pH. *Nucleic Acids Res.*, **33**, 3025–3032.
76. Booher,M.A., Wang,S. and Kool,E.T. (1994) Base pairing and steric interactions between pyrimidine strand bridging loops and the purine strand in DNA pyrimidine.purine.pyrimidine triplexes. *Biochemistry*, **33**, 4645–4651.
77. Povsic,T.J. and Dervan,P.B. (1989) Triple helix formation of oligonucleotides on DNA extended to the physiological range. *J. Am. Chem. Soc.*, **11**, 3059–3061.
78. Janowski,B.A. and Corey,D.R. (2005) Inhibiting transcription of chromosomal DNA using antigene RNAs. *Nucleic Acids Symp. Ser. (Oxf)*, **49**, 367–368.
79. Beane,R.L., Ram,R., Gabillet,S., Arar,K., Monia,B.P. and Corey,D.R. (2007) Inhibiting gene expression with locked nucleic acids (LNAs) that target chromosomal DNA. *Biochemistry*, **46**, 7572–7580.
80. Gagnon,K.T., Watts,J.K., Pendergraff,H.M., Montaillier,C., Thai,D., Potier,P. and Corey,D.R. (2011) Antisense and antigene inhibition of gene expression by cell-permeable oligonucleotide-oligospermine conjugates. *J. Am. Chem. Soc.*, **133**, 8404–8407.